Peroxidasin mediates bromination of tyrosine residues in the extracellular matrix.

Bathish, Boushra; Paumann-Page, Martina; Paton, Louise ; Kettle, Anthony; Winterbourn, Christine

Published in:
Journal of Biological Chemistry

DOI:
10.1074/jbc.RA120.014504

Publication date:
2020

JBC ARTICLE

Peroxidasin mediates bromination of tyrosine residues in the extracellular matrix

Received for publication, May 21, 2020, and in revised form, July 5, 2020 Published, Papers in Press, July 16, 2020, DOI 10.1074/jbc.RA120.014504

Boushra Bathish, Martina Paumann-Page, Louise N. Paton, Anthony J. Kettle, and Christine C. Winterbourn*

From the Centre for Free Radical Research, Department of Pathology and Biomedical Science, University of Otago Christchurch, Christchurch, New Zealand

Edited by Ruma Banerjee

Peroxidasin is a heme peroxidase that oxidizes bromide to hypobromous acid (HOBr), a powerful oxidant that promotes the formation of the sulfilimine crosslink in collagen IV in basement membranes. We investigated whether HOBr released by peroxidasin leads to other oxidative modifications of proteins, particularly bromination of tyrosine residues, in peroxidasin-expressing PFHR9 cells. Using stable isotope dilution LC-MS/MS, we detected the formation of 3-bromotyrosine, a specific biomarker of HOBr-mediated protein modification. The level of 3-bromotyrosine in extracellular matrix proteins from normally cultured cells was 1.1 mmol/mol tyrosine and decreased significantly in the presence of the peroxidasin inhibitor, phloroglucinol. A negligible amount of 3-bromotyrosine was detected in peroxidasin-knockout cells. 3-Bromotyrosine formed both during cell growth in culture and in the isolated decellularized extracellular matrix when embedded peroxidasin was supplied with hydrogen peroxide and bromide. The level of 3-bromotyrosine was significantly higher in extracellular matrix than intracellular proteins, although a low amount was detected intracellularly. 3-Bromotyrosine levels increased with higher bromide concentrations and decreased in the presence of physiological concentrations of thiocyanate and urate. However, these peroxidase substrates showed moderate to minimal inhibition of collagen IV crosslinking. Our findings provide evidence that peroxidasin promotes the formation of 3-bromotyrosine in proteins. They show that HOBr produced by peroxidasin is selective for, but not limited to, the crosslinking of collagen IV. Based on our findings, the use of 3-bromotyrosine as a specific biomarker of oxidative damage by HOBr warrants further investigation in clinical conditions linked to high peroxidasin expression.

Peroxidasin is a heme peroxidase that is widely distributed throughout the animal kingdom (1–3). In mammals, its known physiological function is to catalyze the formation of an essential sulfilimine bond (S=N) between specific methionine and hydroxylysine residues in collagen IV (4). This intermolecular bond is crucial for the functionality and integrity of the basement membrane, a specialized form of the extracellular matrix (ECM). The mechanism involves the oxidation of bromide to hypobromous acid (HOBr), which then promotes the crosslink between specific methionine and hydroxylysine residues in the noncollagenous domain (NCD) to join two protomers of collagen IV (5). Other pathophysiological roles of peroxidasin have been suggested, such as antimicrobial defense (6, 7), redox sensing through interaction with the transcription factor Nrf2 (8), promotion of angiogenesis (9), and kidney fibrosis (10, 11). Homozygous deletion of peroxidasin causes eye defects (12), and high expression has been identified as a determinant of melanoma cell invasion (13).

Mammalian peroxidasin is a typical heme peroxidase that catalyzes the two-electron oxidation of thiocyanate and iodide as well as bromide (14). It also oxidizes typical peroxidase substrates including tyrosine, urate, and nitrite (15). Furthermore, HOBr is a strong oxidant that reacts with numerous biological molecules. Its favored reactions are the oxidation of cysteine and methionine residues and the conversion of amine groups to bromamines (16, 17). HOBr also converts tyrosine to 3-bromotyrosine (3-Br-Tyr) and 3,5-dibromotyrosine at an appreciable rate (16, 18). These brominated products are stable and unique making them ideal biomarkers for detecting the formation of HOBr and its reactions with proteins.

A key question is whether the HOBr produced by peroxidasin forms the collagen IV cross-link exclusively or undergoes other reactions. Our earlier work showed that peroxidasin releases free HOBr as detected by the conversion of added NADH to its bromohydrin (19). Here, by monitoring the formation of 3-Br-Tyr in proteins, we show that the activity of peroxidasin during cell growth and in isolated decellularized ECM leads to HOBr-mediated protein modification. We used mouse epithelial-like PFHR9 cells, which are differentiated embryonal carcinoma cells that secrete appreciable amounts of basement membrane proteins. This cell line has been used in many studies to characterize the cross-linking of collagen IV (4, 20). When PFHR9 cells produce ECM, they secrete peroxidasin which is embedded in the matrix and able to catalyze the formation of the crosslink.

Results

Peroxidasin catalyzes the formation of 3-bromotyrosine during cell growth

As previously reported, PFHR9 cells express peroxidasin, which catalyzes the formation of the sulfilimine crosslink in the collagen IV that they release during the deposition of ECM in culture (4, 19, 21). This unusual crosslink was characterized by Vanacore *et al.* (21) as a linkage between the sulfur of Met^{93} and the amine nitrogen of hydroxy-Lys^{211} in the NCD (Fig. 1*A*). We first confirmed the formation of dimer in the NCD of collagen IV in our system by isolating the ECM after 6–8 days' culture and analyzing the NCD by SDS-PAGE and densitometry

* For correspondence: Christine Winterbourn, christine.winterbourn@otago.ac.nz.

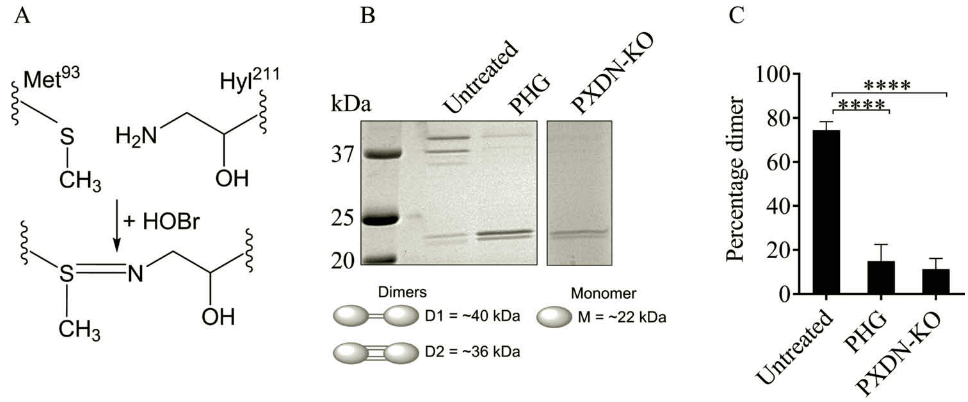

Figure 1. Formation of the sulfilimine crosslinks in the ECM during cell growth in culture. *A*, the structure of the sulfilimine bond between Met[93] and Hyl[211] at the NCD interfaces between two juxtaposed protomers of collagen IV. *B*, formation of dimers in the NCD of collagen IV in ECM isolated from PFHR9 cells cultured for 6–8 days in the absence (*Untreated*) or presence of PHG, or isolated from peroxidasin-knockout PFHR9 cells (PXDN-KO). ECM was digested with collagenase and the NCD was analyzed by SDS-PAGE and Coomassie Brilliant Blue staining. The NCD can be joined by one or two sulfilimine bonds, resulting in two dimers with different electrophoretic mobility: dimer 1 (*upper band*) and dimer 2 (*lower band*). *C*, densitometry analysis of gels from $\geq$3 independent experiments, mean $\pm$ S.D. The percentage of crosslinks was calculated after performing densitometry analysis of the dimers and monomer within each lane as per the equation % Dimer = (D1 + (D2 $\times$ 2))/(D1 + (D2 $\times$ 2) + M) $\times$ 100, where D1 is the density of Dimer 1 (*upper band*) which contains one sulfilimine link and D2 is Dimer 2 (*lower band*) which contains two sulfilimine links, thus is multiplied by 2 to account for both bonds. ****, $p < 0.0001$ by one-way ANOVA analysis followed by Tukey's multiple comparisons.

quantification. The majority (>70%) of the isolated NCD of collagen IV from WT cells was crosslinked (Fig. 1, *B* and *C*). The NCD can be joined by one or two sulfilimine bonds, resulting in two dimers with different electrophoretic mobility: dimer 1 (*upper band*) and dimer 2 (*lower band*) (Fig. 1*B*). Phloroglucinol (PHG) (1,3,5-trihydroxybenzene) is an effective, reversible inhibitor of peroxidasin (22). The crosslinking decreased to ~15% in ECM isolated from WT cells grown in the presence of PHG or from peroxidasin-knockout cells.

We then measured 3-Br-Tyr levels in the ECM from PFHR9 cells cultured under the same conditions. 3-Br-Tyr and Tyr were detected using LC–MS/MS with isotopically labeled internal standards (Fig. 2*A*). As shown in Fig. 2*B*, Tyr and both bromine isotopes of 3-Br-Tyr were detected in ECM from WT cells (*left panel*), whereas the 3-Br-Tyr peaks in ECM isolated from peroxidasin-knockout cells were scarcely detectable (*right panel*). Using the standard calibration curve, the level of 3-Br-Tyr in ECM isolated from the WT cells was calculated to be 1.1 mmol/mol tyrosine and decreased significantly to 0.14 mmol/mol when WT cells were grown in the presence of PHG (Fig. 2*C*). 3-Br-Tyr formation mirrored the profile for dimer formation seen in Fig. 1*C*.

To test substrate requirement for the formation of 3-Br-Tyr during growth of cells, PFHR9 cells were cultured in media supplemented with 50 or 100 μM bromide. It should be noted that a trace amount of bromide (~6 μM in 100 mM NaCl) is present in culture medium as contamination in sodium chloride (5). The level of 3-Br-Tyr increased with increasing bromide concentration and appeared to plateau above 50 μM bromide (Fig. 3*A*). Analysis of dimer formation in the same samples showed that crosslinking was near maximal with the trace amounts of bromide present in the culture medium (Fig. 3*B*).

Levels of 3-bromotyrosine are higher in ECM than in intracellular proteins

To establish whether 3-Br-Tyr is formed on intracellular as well as extracellular proteins, lysates from PFHR9 cells were separated into intracellular extract (ICE), ECM, and NCD. The three fractions were hydrolyzed and analyzed by LC-MS/MS. The level of 3-Br-Tyr detected in the intracellular fraction, (0.13 mmol/mol Tyr) was ~10% of that in the total ECM, whereas the level in the NCD was 1.4-fold higher (Fig. 4). 3-Br-Tyr levels in each fraction increased 1.2- to 1.4-fold when cells were grown in the presence of added bromide and substantially decreased when PHG was present or in ECM from peroxidasin-knockout cells (Table 1).

Formation of 3-bromotyrosine in the isolated decellularized ECM

We also investigated whether peroxidasin embedded in the decellularized ECM promotes 3-Br-Tyr formation. Uncrosslinked ECM was isolated from WT cells grown in the presence of PHG and treated with hydrogen peroxide and bromide. The level of 3-Br-Tyr measured at 1 h increased significantly in the presence of both bromide and hydrogen peroxide, but not when either reagent was added separately (Fig. 5*A*). A similar trend was observed for collagen IV crosslinking (Fig. 5*B*). The levels of 3-Br-Tyr increased progressively over time (Fig. 6*A*), and with increasing concentrations of bromide and hydrogen peroxide (Fig. 6, *B* and *C*). Dimer formation reached near maximal levels at an earlier time point (Fig. 6*D*) and at lower concentrations of bromide and hydrogen peroxide (Fig. 6, *E* and *F*).

Thiocyanate modulates the formation of 3-bromotyrosine

Thiocyanate (SCN^-) is a pseudohalide that competes with bromide as a substrate for peroxidasin (14). Previously, we showed that physiological concentrations of thiocyanate interfere with the crosslinking of collagen IV (19). Here we investigated whether thiocyanate modulates the formation of 3-Br-Tyr. PFHR9 cells were grown in culture medium supplemented with thiocyanate (0–400 μM), either without or with added bromide (50 and 100 μM) to test for substrate competition. The levels of 3-Br-Tyr in ECM isolated from the cells decreased progressively from 1.2 $\pm$ 0.3 to 0.27 $\pm$ 0.03 mmol/mol tyrosine

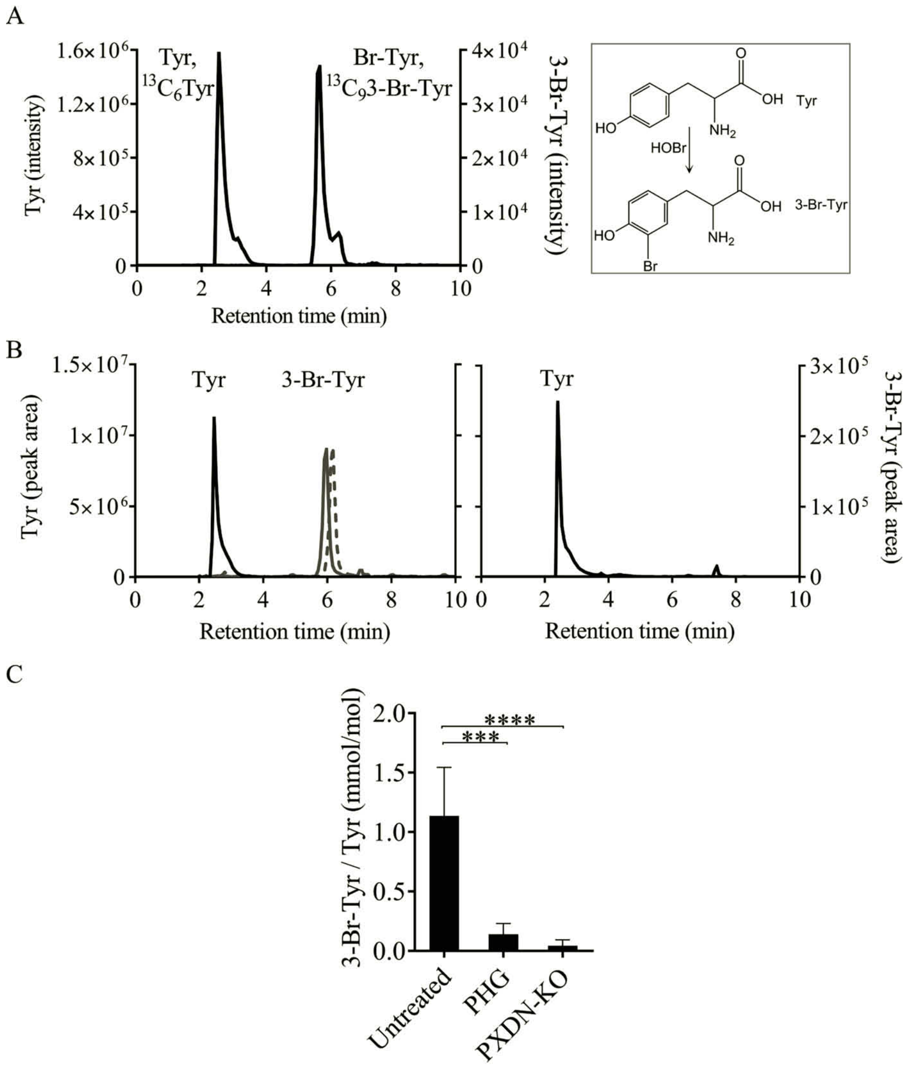

Figure 2. Identification of 3-Br-Tyr in extracellular matrix proteins using LC-MS/MS. *A*, typical LC-MS/MS chromatogram obtained in multiple reaction monitoring mode for the analysis of Tyr and 3-Br-Tyr. The retention time for ^{12}C-Tyr (*m/z* 182 → 136) and isotopically labeled $^{13}C_6$-Tyr (*m/z* 188 → 142) was 2.5 ± 0.2 min. The retention time for the two isotopes 3-^{79}Br-Tyr (*m/z* 260 → 214) and 3-^{81}Br-Tyr (*m/z* 262 → 216) as well as the isotopically labeled internal standards $^{13}C_9$–3-^{79}Br-Tyr (*m/z* 269 → 222) and $^{13}C_9$–3-^{81}Br-Tyr (*m/z* 271 → 224) was 6.0 ± 0.2 min. Artifactual bromination of $^{13}C_6$-Tyr was monitored by measuring $^{13}C_6$–3-^{79}Br-Tyr (*m/z* 266 → 220) and $^{13}C_6$ 3-^{81}Br-Tyr (*m/z* 268 → 222). Chromatograms for isotopically labeled analytes were superimposable on their unlabeled counterparts. The chemical structure of tyrosine and 3-bromotyrosine are shown next to the chromatogram. *B*, representative chromatograms for tyrosine (*solid black line*) and two bromine isotopes of 3-bromotyrosine (*solid gray line* and *dashed gray line*, offset by 0.2 min for visibility) in ECM isolated from WT (*left panel*) or peroxidasin-knockout PFHR9 cells (*right panel*). The ECM samples were hydrolyzed with methane sulfonic acid then analyzed by LC-MS/MS. *C*, the levels of 3-Br-Tyr in ECM isolated from PFHR9 cells cultured for 6–8 days in the absence (*Untreated*) or presence of PHG, or isolated from peroxidasin-knockout PFHR9 cells (PXDN-KO) calculated using standard calibration curves normalized to isotopically labeled internal standards. Values are the means of ≥ 3 independent biological repeats ± S.D. ****, $p < 0.0001$; ***, $p < 0.001$ by one-way ANOVA analysis followed by Tukey's multiple comparisons.

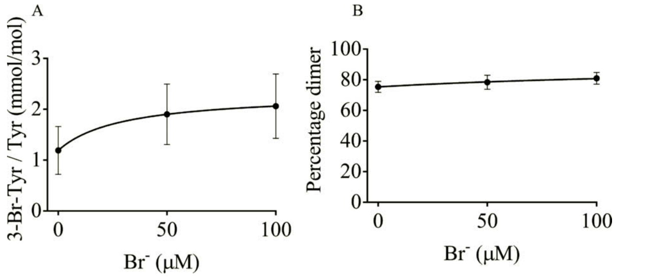

Figure 3. Effect of bromide supplementation on the formation of 3-Br-Tyr and sulfilimine cross-links in the ECM during cell culture. *A*, 3-Br-Tyr and *B*, NCD dimers in ECM isolated from PFHR9 cells cultured for 6–8 days with the indicated concentrations of bromide. Samples were analyzed as described in Figs. 1 and 2. Values are the means of ≥ 3 independent biological repeats ± S.D. *Curves* represent nonlinear regression lines selected to give best fit to the experimental data points.

with increasing concentration of thiocyanate in the medium (Fig. 7*A*). Supplementing the medium with bromide increased the starting level of 3-Br-Tyr and the IC_{50} for inhibition by thiocyanate. Dimer formation in the NCD was also progressively inhibited by increasing thiocyanate concentration but to a lesser extent than tyrosine bromination (Fig. 7*B*).

We also studied the effect of thiocyanate in the isolated ECM system. Uncrosslinked ECM from PFHR9 cells grown in the presence of PHG was decellularized and treated with increasing concentrations of thiocyanate (0–400 μM), in addition to bromide (50 or 100 μM) and 50 μM hydrogen peroxide. Similar to the results in the cell culture system, bromination of tyrosine residues in decellularized isolated ECM decreased with increasing concentration of thiocyanate,

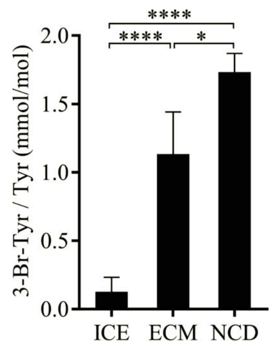

Figure 4. Levels of 3-bromotyrosine in ICE, ECM, and NCD. Cells were cultured for 6–8 days in medium alone. All samples were hydrolyzed and analyzed by LC-MS/MS as described in Fig. 2. Values are the means of 4–5 independent experiments ± S.D. *, $p < 0.05$; ****, $p < 0.0001$ by one-way ANOVA analysis followed by Tukey's multiple comparisons.

Table 1
Levels of 3-Br-Tyr in ICE, ECM, and NCD

PFHR9 cells were grown in cell culture with medium alone (Untreated), 100 μM bromide (+Br^-), and 50 μM phloroglucinol (+PHG). Peroxidasin-knockout cells (KO) were grown in cell culture medium alone. Samples were analyzed as described in Fig. 2. Values are the means of four independent experiments ± S.E. *, $p < 0.05$; **, $p < 0.01$; ****, $p < <0.0001$ by one-way ANOVA analysis followed by Tukey's multiple comparisons of each treatment of the WT cells to the untreated respective fraction.

	ICE	ECM (mmol 3-Br-Tyr/mol Tyr)	NCD
Untreated	0.13 ± 0.05	1.13 ± 0.15	1.73 ± 0.08
+ Br^-	0.19 ± 0.07	1.54 ± 0.26	2.13 ± 0.51
+ PHG	0.04 ± 0.01	0.14 ± 0.05*	0.34 ± 0.08****
KO	0.03 ± 0.02	0.03 ± 0.00*	0.12 ± 0.01**

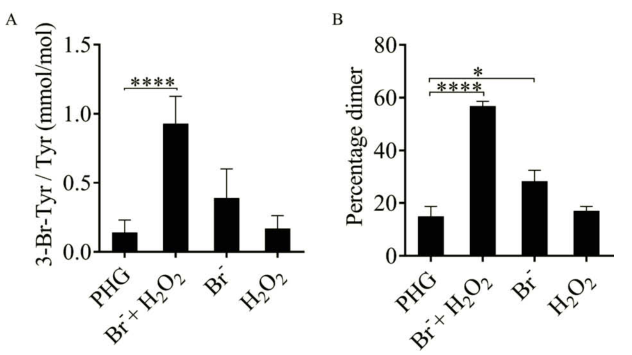

Figure 5. Formation of 3-Br-Tyr and sulfilimine crosslinks in decellularized ECM. *A*, 3-Br-Tyr and *B*, NCD dimer in ECM isolated from cells grown in the presence of PHG was treated with 100 μM Br^- and/or 50 μM H_2O_2 for 1 h at 37°C. Samples were analyzed as described in Figs. 1 and 2. Values are the means of ≥ 3 independent biological repeats ± S.D. *, $p < 0.05$; ****; $p < 0.0001$ by one-way ANOVA analysis followed by Tukey's multiple comparisons.

with near complete inhibition at 400 μM (Fig. 7*C*). Increasing the bromide concentration also led to a higher IC_{50}. Thiocyanate also caused a decline in dimer formation but to a much lesser extent than the inhibition of 3-Br-Tyr formation (Fig. 7*D*).

In earlier work, we showed that urate modulates the formation of the sulfilimine crosslink in collagen IV (19). Here we tested whether it also affects the formation of 3-Br-Tyr. When added to culture medium without added bromide, up to 400 μM urate caused a gradual decline in 3-Br-Tyr in the ECM, from 1.2 ± 0.2 to 0.68 ± 0.2 mmol/mol Tyr. When 100 μM bromide was also added, the level of 3-Br-Tyr decreased from 1.7 ± 0.3 to 1.3 ± 0.3 mmol/mol Tyr. In contrast to the inhibition of dimer formation in the decellularized ECM system, urate scarcely affected dimer formation in cell culture, with no observable inhibition in the presence of 100 μM bromide (data not shown).

Discussion

We have demonstrated that HOBr produced by peroxidasin leads to the formation of 3-Br-Tyr residues in extracellular proteins as well as promoting sulfilimine crosslinks in collagen IV. We show that bromination occurs during growth of epithelial-like cells in culture, as well as in isolated decellularized ECM. That peroxidasin is responsible for the formation of 3-Br-Tyr is evident from the very low level measured in ECM isolated from peroxidasin-knockout cells and the strong inhibitory effect of PHG. Therefore, peroxidasin activity is not restricted to forming the sulfilimine crosslink in collagen IV but also causes other protein modifications.

In cell culture, the level of 3-Br-Tyr increased with increasing bromide concentration, but with no added bromide the extent of bromination was already about half maximal. As observed previously (19), sulfilimine formation was maximal without the addition of bromide. This can be accounted for by the trace amounts of bromide present in the culture medium (5). Our findings indicate that the HOBr produced by peroxidasin shows a degree of selectivity for the crosslinking of collagen IV but even at low concentrations of bromide, there is substantial 3-Br-Tyr formation. At higher concentrations, but still within the physiological range of 20–100 μM, production of HOBr and its reactions with other targets are increased.

3-Br-Tyr was also produced in isolated decellularized ECM, when supplied with the peroxidasin substrates bromide and hydrogen peroxide. Levels of 3-Br-Tyr were in the same range as those formed during cell growth in culture, but added bromide was required and the concentration dependence was more pronounced. The isolated ECM also required a higher bromide concentration for maximal dimer formation. This difference might be because of the longer time in cell culture allowing accumulation of 3-Br-Tyr and NCD dimer. Another possibility is that the cellular system binds or concentrates bromide to a higher effective concentration than that of the medium and this compartmentalization is lost during isolation of the ECM. It is also possible that steric specificity conferred by peroxidasin-binding partners is lost during processing.

To determine the location of brominated proteins following cell culture, ICE, which would contain membrane and organelle as well as cytoplasmic proteins, total ECM, and the NCD of collagen IV were examined. On a 3-Br-Tyr per Tyr basis, the ECM proteins showed much higher bromination. This is consistent with peroxidasin catalyzing bromination once secreted to the ECM, where it has been shown to catalyze the crosslinking of collagen IV (4). It is possible that some activity could occur before secretion. A low but significant amount of 3-Br-Tyr was detected in the intracellular extract. It is unlikely to be because of contamination with ECM proteins, as approximately six times more protein was extracted in the ICE than

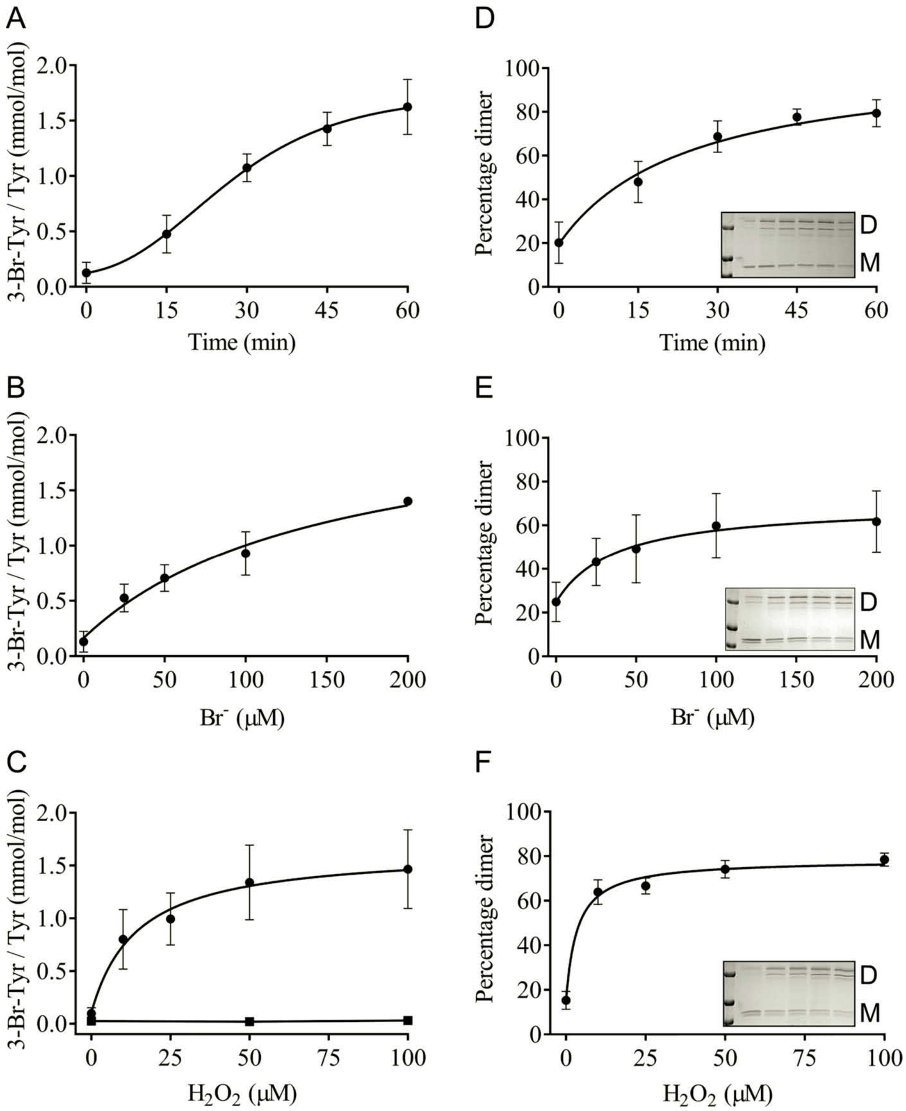

Figure 6. Effects of incubation time and the concentrations of bromide and hydrogen peroxide on the formation of 3-Br-Tyr and sulfilimine cross-links in decellularized ECM. *A–C*, 3-Br-Tyr, and *D–F*, NCD dimer in ECM isolated from cells grown in the presence of PHG for 6–8 days was treated at 37°C with (*A* and *D*) 50 μM H_2O_2 and 100 μM Br^- for the indicated time, (*B* and *E*) 50 μM H_2O_2 and the indicated concentrations of Br^- for 1 h, or (*C* and *F*) 100 μM Br^- and the indicated concentrations of H_2O_2 for 1 h. ECM from WT (*filled black circle*), peroxidasin-knockout cells (*filled black squares*) was analyzed as described in Figs. 1 and 2. *Insets* are representative gel images of NCD resolved by SDS-PAGE and visualized by Coomassie Brilliant Blue staining. First lane shows 37, 25, and 20 kDa markers as in Fig. 1*B*, with subsequent lanes showing sequence of sample analyses as in main figures. Values represent the means of three independent experiments ± S.D. *Error bars* are not visible when they were within the symbol size. *Curves* represent nonlinear regression lines selected to give best fit to the experimental data points.

the ECM and to achieve the observed level of 3-Br-Tyr in the ICE fraction would require half of the total ECM protein to have been solubilized into the ICE. Peroxidasin has been detected in the endoplasmic reticulum where it is synthesized, processed, and secreted via the Golgi (1, 23), then cleaved by proprotein convertase A at the cell membrane (24). These organelles are possible sites for intracellular 3-Br-Tyr formation but further fractionation is required to establish whether this is the case.

The level of 3-Br-Tyr was significantly higher in the NCD of collagen IV than in the total ECM. To assess whether all the 3-Br-Tyr could reside in the NCD, we considered that the NCD constitutes ~7% of the total ECM protein (~14% of the amino acids in collagen IV, which accounts for ~50% of the structural proteins in basement membranes) (25–27). As the 3-Br-Tyr:Tyr ratio was only 1.4-fold higher in the NCD, the small fraction of NCD cannot account for the bromination of tyrosine in the ECM. Therefore, although the sulfilimine crosslinking by the HOBr produced by peroxidasin occurs specifically in the NCD of collagen IV, other reactions of HOBr are not restricted to this region. During submission of this manuscript, He *et al.* (28) reported MS evidence for peroxidasin-mediated bromine enrichment in kidney basement membranes, corroborating our findings of 3-Br-Tyr in ECM. They detected bromination of a particular Tyr residue in the collagen IV NCD, but as shown here, bromination is not restricted to this region.

Thiocyanate is a better peroxidasin substrate than bromide, with rate constants of 1.83×10^7 and 5.6×10^6 M^{-1} s^{-1}, respectively, having been measured for reaction with compound I of a truncated recombinant form that contains the

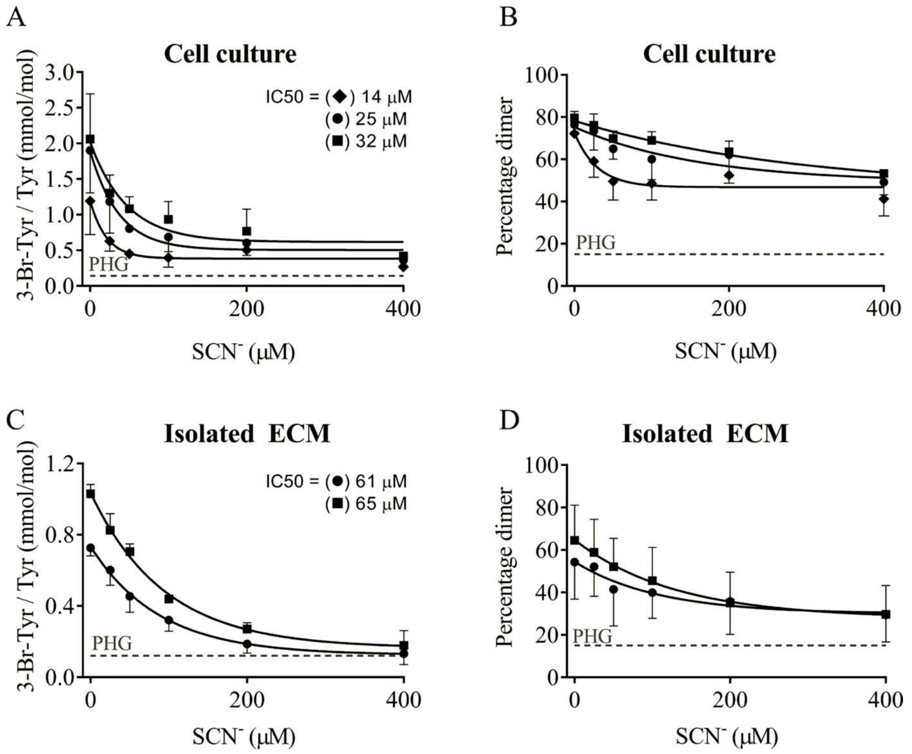

Figure 7. Effects of thiocyanate on the formation of 3-Br-Tyr and sulfimine crosslinks. *A*, 3-Br-Tyr and *B*, NCD dimer in PFHR9 cells cultured for 6–8 days in the presence of varying concentrations of SCN^- either without added Br^- (*filled black diamond*) or with 50 μM (*filled black circle*) or 100 μM Br^- (*filled black square*) added. *C*, 3-Br-Tyr and *D*, NCD dimers, ECM isolated from PFHR9 cells cultured in the presence of PHG was treated with 50 μM H_2O_2 and 50 μM (*filled black circle*) or 100 μM (*filled black square*) Br^-, plus the indicated concentrations of SCN^- for 1 h at 37°C. 3-Br-Tyr and dimer analyses were performed as described in Figs. 1 and 2. Values represent the means of three independent biological repeats ± S.D. The *gray dashed lines* represent inhibition by 50 μM PHG. IC_{50} values were calculated from exponential decay curves in each figure. *Error bars* are shown in one direction for clarity and are not visible when they are within the symbol size. *Curves* represent nonlinear regression lines selected to give best fit to the experimental data points.

peroxidase and Ig domains (14). The product of thiocyanate oxidation, HOSCN, does not crosslink collagen thiocyanate inhibits crosslinking (5, 19), as recapitulated here. The extent of inhibition is less than might be expected from the above rate constants, suggesting that peroxidasin may have an affinity for bromide, possibly because of location and association with ECM proteins. In the present study thiocyanate inhibited 3-Br-Tyr formation more effectively than collagen IV crosslinking, either when added to cells in culture or to isolated ECM. The observed IC_{50} values and their increase with increasing bromide concentration imply that thiocyanate acts as a competitive substrate. However, thiocyanate reacts rapidly with HOBr (a rate constant of 2.3×10^9 compared with 2.6×10^5 M^{-1} s^{-1} for tyrosine) (17, 29) and could also inhibit bromination by direct scavenging. Either way, our results indicate that the reactions of peroxidasin-derived HOBr could be modulated by physiological levels of thiocyanate, which are typically 20–120 μM. As HOSCN is less reactive than HOBr (30, 31), high thiocyanate concentrations could be advantageous in protecting from the harmful, presumably collateral, effects of HOBr without compromising the sulfilimine crosslink.

Peroxidasin reacts with a range of peroxidase substrates, including urate (15). Urate inhibited bromination activity by the recombinant enzyme (15) and partially inhibited crosslinking in isolated ECM (19). With cultured cells we observed little inhibition of crosslinking or 3-Br-Tyr formation by urate at high physiological concentrations, suggesting the relevance of such inhibition is likely to be minor.

The level of bromination that we detected in ECM proteins was around one in a thousand tyrosines. Although this may seem low, similar levels have been observed in experimental and clinical studies of eosinophil peroxidase (18, 32). Furthermore, although 3-Br-Tyr is a good biomarker for HOBr, cysteine, methionine, tryptophan, histidine, and α-amino groups are more favored targets than tyrosine (16, 17). Peroxidasin can also catalyze dityrosine formation (3). Therefore, the detection of 3-Br-Tyr is an indication that more extensive modifications to protein, and potentially other biomolecules, are likely to occur. The nature of such modifications and their implications need to be established.

Our finding that peroxidasin activity yields 3-Br-Tyr has implications for clinical studies where 3-Br-Tyr has been measured in body fluids and tissues and used as a biomarker of oxidative damage in pathological conditions including asthma, sinonasal inflammation, cystic fibrosis, eosinophilic esophagitis, and diabetes (32–37). In such studies, the formation of 3-Br-Tyr has been attributed to other heme peroxidases, namely myeloperoxidase and eosinophil peroxidase (18, 32, 38). Our findings raise the possibility that it arises from peroxidasin activity. Peroxidasin is widely expressed in human tissues, including the vascular system (39), with high expression in some cancer cells (13, 40). It could act as a resident contributor to oxidative damage of proteins in the ECM, a tissue with poor antioxidant defense. Pro-oxidant activity of peroxidasin has been proposed to play a role in hypertension and ischemia-reperfusion injury (41–45), and evidence that halogenation of ECM proteins impairs renal function in a mouse

 ASBMB

model suggests that it might be involved in diabetic glomerular injury (42). Furthermore, tyrosine halogenation decreases the pK_a of the phenol group (46), which can affect tyrosine phosphorylation and consequently cell signaling cascades. Therefore, tyrosine bromination by peroxidasin might have a wide impact, especially given the role of the ECM in cell signaling (47).

In summary, we have used 3-Br-Tyr as a specific biomarker to show that the reactions of HOBr produced by peroxidasin are not limited to the crosslinking of collagen IV. Further research is needed to characterize the structural and functional impact of HOBr in peroxidasin-producing cells. Our findings also raise questions about the origin of 3-Br-Tyr in clinical material and open the door to investigating the role of peroxidasin in catalyzing oxidative modifications in pathological conditions.

Experimental Procedures

Materials

DMEM and fetal bovine serum were obtained from Gibco/Life Technologies, hydrogen peroxide from LabServ, sodium hypochlorite (Janola) from Pental Products, bacterial collagenase from Worthington, and phloroglucinol (1,3,5-trihydroxybenzene) from Sigma Aldrich. Other chemicals were obtained from Sigma Aldrich, BDH Chemicals, or JT Baker.

Mouse epithelial-like cells PFHR9 (ATCC CLR-2423) were obtained from the American Type Culture Collection. Peroxidasin-knockout PFHR9 cells were generated using CRISPR-Cas9 gene editing, as described by Colon and Bhave (24) and generously donated by Dr. Gautam Bhave from Vanderbilt University, Nashville, Tennessee.

Cell culture and isolation of ECM

We followed the method described by Bhave *et al.* (4). Briefly, PFHR9 cells were seeded at high density ($\sim 9 \times 10^6$ cells in a 15-cm culture plate) and grown in DMEM (plus 10% fetal bovine serum) for 6–8 days post confluency to deposit the ECM. The medium was changed daily with supplementation of 50 μM PHG, potassium bromide, or sodium thiocyanate as indicated. The cells were lysed with ice cold lysis buffer (10 mM Tris, pH 8, 1 mM EDTA, 1% sodium deoxycholate, 1 × cOmplete® Protease Inhibitor), scraped, sonicated until homogeneous, and centrifuged at $20{,}000 \times g$ to separate the supernatant, designated ICE, from the ECM pellet. The pellet was washed twice in Wash Buffer (1M NaCl, 10 mM Tris, pH 7.5) with centrifugation and resuspended in PBS with brief sonication. Protein concentration was measured using the Direct Detect® IR Spectrometer. The yield of ECM proteins from a 15-cm culture plate after 6–8 days was ~5 mg. Established procedures were used to separate the noncollagenous domain. Isolated ECM was resuspended in digestion buffer (2 mg/ml bacterial collagenase in 50 mM sodium phosphate, pH 7.4) and left overnight at 37°C (48). The NCD was purified by anion-exchange chromatography using DEAE-resin (49). The soluble digest was mixed with an equal volume of DEAE-resin (equilibrated in 50 mM Tris, pH 7.4) with shaking for 1 h at 4°C. The slurry was centrifuged and the soluble unbound NCD in the supernatant was used for analysis. The purified NCD was resolved by SDS-PAGE and stained with Coomassie Brilliant Blue R-250.

Treatment of the isolated decellularized ECM

ECM isolated from cells grown in the presence of 50 μM PHG was resuspended in PBS and sonicated. Potassium bromide and hydrogen peroxide (concentrations indicated in each figure) were added to 350 μg of ECM protein in a total volume of 300 μl. The reaction was carried out at 37°C for 60 min (unless stated otherwise) and stopped by adding 1 mM azide or 5 mM methionine. Other substrates and inhibitors were added at the concentrations stated in each figure.

Detection of 3-bromotyrosine

A stable isotope dilution LC-MS/MS method was used for the detection and quantification of 3-Br-Tyr levels in proteins as described previously (18, 33, 50, 51). Isotopically labeled standards ($^{13}C_6$-Tyr and $^{13}C_9$–3-Br-Tyr) were used to control for experimental variations, such as recovery, matrix effect, and ionization. Artifactual bromination was monitored by measuring any conversion of $^{13}C_6$-Tyr to $^{13}C_6$–3-Br-Tyr and was minimal. The two bromotyrosine isotopes (*m/z* 260 for the ^{79}Br-containing isotope and *m/z* 262 for the ^{81}Br-containing isotope) occurred at 1:1 ratio and their peak areas were summed for quantification. A typical chromatogram is shown in Fig. 2*A*. Standard calibration curves using the ratios ^{12}C-Tyr:$^{13}C_6$-Tyr and ^{12}C–Br-Tyr:$^{13}C_9$–Br-Tyr were used for quantification.

Protein samples (50 μg) were hydrolyzed with internal standards (6 nmol $^{13}C_6$-Tyr and 6 pmol $^{13}C_9$–3-Br-Tyr) in 4 M methane sulfonic acid, supplemented with 1% (w/v) phenol, under nitrogen at 110°C for 18 h. The hydrolysate was processed by solid phase extraction to remove the acid and eluted with 80% (v/v) methanol. Eluents were dried and reconstituted in 0.1% (v/v) formic acid for analysis. Reverse-phase HPLC-MS/MS was performed using a Kinetex® 2.6 μM C18 100-Å column (150 × 2.1 mm) and an Agilent 1290 Binary Pump at a flow rate of 200 μl/min. The gradient started with 2% acetonitrile with 0.1% (v/v) formic acid for 4 min, increased to 80% acetonitrile over 3 min, maintained this over 3 min then equilibrated with the starting eluent. The analytes were delivered into a Qtrap® 6500 mass spectrometer (Sciex) and detected in multiple reaction monitoring mode using positive ion mode. The ion spray was set to 5.5 kV and the temperature was set to 600°C. The collision gas was nitrogen and the collision energy was 25%. The areas of peaks were calculated using Analyst Software v 1.6.2 (Sciex). A linear response was observed over the range 0.1–10 nmol for tyrosine and 0.1–10 pmol for 3-bromotyrosine.

Data availability

All data are available within the manuscript.

Acknowledgments—We are grateful to Dr. Rufus Turner for assistance with the mass spectrometry and Dr. Gautam Bhave from Vanderbilt University for the peroxidasin-knockout cell line.

Author contributions—B. B. and M. P.-P. investigation; B. B. and L. N. P. methodology; B. B. writing-original draft; M. P.-P., A. J. K., and C. C. W. writing-review and editing; A. J. K. and C. C. W.

supervision; C. C. W. conceptualization; A. J. K. and C. C. W. funding acquisition.

Funding and additional information—This work was supported by a New Zealand Marsden Fund grant (to A. J. K. and C. C. W.).

Conflict of interest—The authors declare that they have no conflicts of interest with the contents of this article.

Abbreviations—The abbreviations used are: ANOVA, analysis of variance; 3-Br-Tyr, 3-bromotyrosine; ECM, extracellular matrix; ICE, intracellular extract; NCD, noncollagenous domain; PHG, phloroglucinol.

References

1. Lázár, E., Péterfi, Z., Sirokmány, G., Kovács, H. A., Klement, E., Medzihradszky, K. F., and Geiszt, M. (2015) Structure-function analysis of peroxidasin provides insight into the mechanism of collagen IV crosslinking. *Free Radic. Biol. Med.* **83,** 273–282 CrossRef Medline
2. Soudi, M., Zamocky, M., Jakopitsch, C., Furtmüller, P. G., and Obinger, C. (2012) Molecular evolution, structure, and function of peroxidasins. *Chem. Biodivers.* **9,** 1776–1793 CrossRef Medline
3. Nelson, R. E., Fessler, L. I., Takagi, Y., Blumberg, B., Keene, D. R., Olson, P. F., Parker, C. G., and Fessler, J. H. (1994) Peroxidasin: A novel enzyme–matrix protein of Drosophila development. *EMBO J.* **13,** 3438–3447 CrossRef Medline
4. Bhave, G., Cummings, C. F., Vanacore, R. M., Kumagai-Cresse, C., Ero-Tolliver, I. A., Rafi, M., Kang, J. S., Pedchenko, V., Fessler, L. I., Fessler, J. H., and Hudson, B. G. (2012) Peroxidasin forms sulfilimine chemical bonds using hypohalous acids in tissue genesis. *Nat. Chem. Biol.* **8,** 784–790 CrossRef Medline
5. McCall, A. S., Cummings, C. F., Bhave, G., Vanacore, R., Page-McCaw, A., and Hudson, B. G. (2014) Bromine is an essential trace element for assembly of collagen IV scaffolds in tissue development and architecture. *Cell* **157,** 1380–1392 CrossRef Medline
6. Li, H., Cao, Z., Moore, D. R., Jackson, P. L., Barnes, S., Lambeth, J. D., Thannickal, V. J., and Cheng, G. (2012) Microbicidal activity of vascular peroxidase 1 in human plasma via generation of hypochlorous acid. *Infect. Immun.* **80,** 2528–2537 CrossRef Medline
7. Shi, R., Cao, Z., Li, H., Graw, J., Zhang, G., Thannickal, V. J., and Cheng, G. (2018) Peroxidasin contributes to lung host defense by direct binding and killing of gram-negative bacteria. *PLoS Pathog.* **14,** e1007026 CrossRef Medline
8. Hanmer, K. L., and Mavri-Damelin, D. (2018) Peroxidasin is a novel target of the redox-sensitive transcription factor Nrf2. *Gene* **674,** 104–114 CrossRef Medline
9. Medfai, H., Khalil, A., Rousseau, A., Nuyens, V., Paumann-Page, M., Sevcnikar, B., Furtmüller, P. G., Obinger, C., Moguilevsky, N., Peulen, O., Herfs, M., Castronovo, V., Amri, M., Van Antwerpen, P., Vanhamme, L., *et al.* (2018) Human peroxidasin 1 promotes angiogenesis through ERK1/2, Akt and FAK pathways. *Cardiovasc. Res.* **115,** 463–475 CrossRef Medline
10. McCall, A. S., Bhave, G., Pedchenko, V., Hess, J., Free, M., Little, D. J., Baker, T. P., Pendergraft, W. F., 3rd, Falk, R. J., Olson, S. W., and Hudson, B. G. (2018) Inhibitory anti-peroxidasin antibodies in pulmonary-renal syndromes. *J. Am. Soc. Nephrol.* **29,** 2619–2625 CrossRef Medline
11. Bhave, G., Colon, S., and Ferrell, N. (2017) The sulfilimine cross-link of collagen IV contributes to kidney tubular basement membrane stiffness. *Am. J. Physiol. Renal Physiol.* **313,** F596–F602 CrossRef Medline
12. Khan, K., Rudkin, A., Parry, D. A., Burdon, K. P., McKibbin, M., Logan, C. V., Abdelhamed, Z. I., Muecke, J. S., Fernandez-Fuentes, N., Laurie, K. J., Shires, M., Fogarty, R., Carr, I. M., Poulter, J. A., Morgan, J. E., *et al.* (2011) Homozygous mutations in PXDN cause congenital cataract, corneal opacity, and developmental glaucoma. *Am. J. Hum. Genet.* **89,** 464–473 CrossRef Medline
13. Jayachandran, A., Prithviraj, P., Lo, P. H., Walkiewicz, M., Anaka, M., Woods, B. L., Tan, B., Behren, A., Cebon, J., and McKeown, S. J. (2016) Identifying and targeting determinants of melanoma cellular invasion. *Oncotarget* **7,** 41186–41202 CrossRef Medline
14. Paumann-Page, M., Katz, R. S., Bellei, M., Schwartz, I., Edenhofer, E., Sevcnikar, B., Soudi, M., Hofbauer, S., Battistuzzi, G., Furtmüller, P. G., and Obinger, C. (2017) Pre-steady-state kinetics reveal the substrate specificity and mechanism of halide oxidation of truncated human peroxidasin 1. *J. Biol. Chem.* **292,** 4583–4592 CrossRef Medline
15. Sevcnikar, B., Paumann-Page, M., Hofbauer, S., Pfanzagl, V., Furtmüller, P. G., and Obinger, C. (2020) Reaction of human peroxidasin 1 compound I and compound II with one-electron donors. *Arch. Biochem. Biophys.* **681,** 108267 CrossRef Medline
16. Pattison, D. I., and Davies, M. J. (2004) Kinetic analysis of the reactions of hypobromous acid with protein components. *Biochemistry* **43,** 4799–4809 CrossRef Medline
17. Pattison, D. I., and Davies, M. J. (2006) Reactions of myeloperoxidase-derived oxidants with biological substrates: Gaining chemical insight into human inflammatory diseases. *Curr. Med. Chem.* **13,** 3271–3290 CrossRef Medline
18. Wu, W., Chen, Y., d'Avignon, A., and Hazen, S. L. (1999) 3-Bromotyrosine and 3,5-dibromotyrosine are major products of protein oxidation by eosinophil peroxidase: Potential markers for eosinophil-dependent tissue injury in vivo. *Biochem. J.* **38,** 3538–3548 CrossRef Medline
19. Bathish, B., Turner, R., Paumann-Page, M., Kettle, A. J., and Winterbourn, C. C. (2018) Characterisation of peroxidasin activity in isolated extracellular matrix and direct detection of hypobromous acid formation. *Arch. Biochem. Biophys.* **646,** 120–127 CrossRef Medline
20. Sirokmány, G., Kovács, H. A., Lázár, E., Kónya, K., Donkó, Á., Enyedi, B., Grasberger, H., and Geiszt, M. (2018) Peroxidasin-mediated crosslinking of collagen IV is independent of NADPH oxidases. *Redox Biol.* **16,** 314–321 CrossRef Medline
21. Vanacore, R. M., Ham, A. J. L., Voehler, M., Sanders, C. R., Conrads, T. P., Veenstra, T. D., Sharpless, K. B., Dawson, P. E., and Hudson, B. G. (2009) A sulfilimine bond identified in collagen IV. *Science* **325,** 1230–1234 CrossRef Medline
22. Balls, A. K., and Hale, W. S. (1934) On peroxidase. *J. Biol. Chem.* **107,** 767–783
23. Péterfi, Z., Donkó, A., Orient, A., Sum, A., Prókai, A., Molnár, B., Veréb, Z., Rajnavölgyi, E., Kovács, K. J., Müller, V., Szabó, A. J., and Geiszt, M. (2009) Peroxidasin is secreted and incorporated into the extracellular matrix of myofibroblasts and fibrotic kidney. *Am. J. Pathol.* **175,** 725–735 CrossRef Medline
24. Colon, S., and Bhave, G. (2016) Proprotein Convertase Processing Enhances Peroxidasin Activity to Reinforce Collagen IV. *J. Biol. Chem.* **291,** 24009–24016 CrossRef Medline
25. Timpl, R., Wiedemann, H., van Delden, V., Furthmayr, H., and Kühn, K. (1981) A network model for the organization of type IV collagen molecules in basement membranes. *Eur. J. Biochem.* **120,** 203–211 CrossRef Medline
26. Sundaramoorthy, M., Meiyappan, M., Todd, P., and Hudson, B. G. (2002) Crystal structure of NC1 domains. Structural basis for type IV collagen assembly in basement membranes. *J. Biol. Chem.* **277,** 31142–31153 CrossRef Medline
27. Muthukumaran, G., Blumberg, B., and Kurkinen, M. (1989) The complete primary structure for the alpha 1-chain of mouse collagen IV. Differential evolution of collagen IV domains. *J. Biol. Chem.* **264,** 6310–6317 Medline
28. He, C., Song, W., Weston, T. A., Tran, C., Kurtz, I., Zuckerman, J. E., Gagliardo, P., Miner, J. H., Ivanov, S. V., Bougoure, J., Hudson, B. G., Colon, S., Voziyan, P. A., Bhave, G., Fong, L. G., *et al.* (2020) Peroxidasin-mediated bromine enrichment of basement membranes. *Proc. Natl. Acad. Sci. U. S. A.* **117,** 15827–15836 CrossRef Medline
29. Nagy, P., Beal, J. L., and Ashby, M. T. (2006) Thiocyanate is an efficient endogenous scavenger of the phagocytic killing agent hypobromous acid. *Chem. Res. Toxicol.* **19,** 587–593 CrossRef Medline
30. O'Brien, P. J. (2000) Peroxidases. *Chem. Biol. Interact.* **129,** 113–139 CrossRef Medline

31. Hawkins, C. L. (2009) The role of hypothiocyanous acid (HOSCN) in biological systems. *Free Radic. Res.* **43,** 1147–1158 CrossRef Medline
32. Wu, W., Samoszuk, M. K., Comhair, S. A., Thomassen, M. J., Farver, C. F., Dweik, R. A., Kavuru, M. S., Erzurum, S. C., and Hazen, S. L. (2000) Eosinophils generate brominating oxidants in allergen-induced asthma. *J. Clin. Invest.* **105,** 1455–1463 CrossRef Medline
33. Aldridge, R. E., Chan, T., van Dalen, C. J., Senthilmohan, R., Winn, M., Venge, P., Town, G. I., and Kettle, A. J. (2002) Eosinophil peroxidase produces hypobromous acid in the airways of stable asthmatics. *Free Radic. Biol. Med.* **33,** 847–856 CrossRef Medline
34. Thomson, E., Brennan, S., Senthilmohan, R., Gangell, C. L., Chapman, A. L., Sly, P. D., Kettle, A. J., Australian Respiratory Early Surveillance Team For Cystic Fibrosis (AREST CF), Balding, E., Berry, L. J., Carlin, J. B., Carzino, R., de Klerk, N., Douglas, T., Foo, C., *et al.* (2010) Identifying peroxidases and their oxidants in the early pathology of cystic fibrosis. *Free Radic. Biol. Med.* **49,** 1354–1360 CrossRef Medline
35. Citardi, M. J., Song, W., Batra, P. S., Lanza, D. C., and Hazen, S. L. (2006) Characterization of oxidative pathways in chronic rhinosinusitis and sinonasal polyposis. *Am. J. Rhinol.* **20,** 353–359 CrossRef Medline
36. Kato, Y., Dozaki, N., Nakamura, T., Kitamoto, N., Yoshida, A., Naito, M., Kitamura, M., and Osawa, T. (2009) Quantification of modified tyrosines in healthy and diabetic human urine using liquid chromatography/tandem mass spectrometry. *J. Clin. Biochem. Nutr.* **44,** 67–78 CrossRef Medline
37. Wedes, S. H., Wu, W., Comhair, S. A., McDowell, K. M., DiDonato, J. A., Erzurum, S. C., and Hazen, S. L. (2011) Urinary bromotyrosine measures asthma control and predicts asthma exacerbations in children. *J. Pediatr.* **159,** 248–255.e241 CrossRef Medline
38. Senthilmohan, R., and Kettle, A. J. (2006) Bromination and chlorination reactions of myeloperoxidase at physiological concentrations of bromide and chloride. *Arch. Biochem. Biophys.* **445,** 235–244 CrossRef Medline
39. Cheng, G., Li, H., Cao, Z., Qiu, X., McCormick, S., Thannickal, V. J., and Nauseef, W. M. (2011) Vascular peroxidase-1 is rapidly secreted, circulates in plasma, and supports dityrosine cross-linking reactions. *Free Radic. Biol. Med.* **51,** 1445–1453. CrossRef Medline
40. Zheng, Y. Z., and Liang, L. (2018) High expression of PXDN is associated with poor prognosis and promotes proliferation, invasion as well as migration in ovarian cancer. *Ann. Diagn. Pathol.* **34,** 161–165 CrossRef Medline
41. Yang, L., Bai, Y., Li, N., Hu, C., Peng, J., Cheng, G., Zhang, G., and Shi, R. (2013) Vascular VPO1 expression is related to the endothelial dysfunction in spontaneously hypertensive rats. *Biochem. Biophys. Res. Commun.* **439,** 511–516 CrossRef Medline
42. Brown, K, L., Darris, C., Rose, K. L., Sanchez, O. A., Madu, H., Avance, J., Brooks, N., Zhang, M. Z., Fogo, A., Harris, R., Hudson, B. G., and Voziyan, P. (2015) Hypohalous acids contribute to renal extracellular matrix damage in experimental diabetes. *Diabetes* **64,** 2242–2253 CrossRef Medline
43. Li, T. T., Zhang, Y. S., He, L., Liu, B., Shi, R. Z., Zhang, G. G., and Peng, J. (2012) Inhibition of vascular peroxidase alleviates cardiac dysfunction and apoptosis induced by ischemia-reperfusion. *Can. J. Physiol. Pharmacol.* **90,** 851–862 CrossRef Medline
44. Ma, Q. L., Zhang, G. G., and Peng, J. (2013) Vascular peroxidase 1: A novel enzyme in promoting oxidative stress in cardiovascular system. *Trends Cardiovasc. Med.* **23,** 179–183 CrossRef Medline
45. Zhang, Y. S., He, L., Liu, B., Li, N. S., Luo, X. J., Hu, C. P., Ma, Q. L., Zhang, G. G., Li, Y. J., and Peng, J. (2012) A novel pathway of NADPH oxidase/vascular peroxidase 1 in mediating oxidative injury following ischemia-reperfusion. *Basic Res. Cardiol.* **107,** 266 CrossRef Medline
46. Yu, Y., Lv, X., Li, J., Zhou, Q., Cui, C., Hosseinzadeh, P., Mukherjee, A., Nilges, M. J., Wang, J., and Lu, Y. (2015) Defining the role of tyrosine and rational tuning of oxidase activity by genetic incorporation of unnatural tyrosine analogs. *J. Am. Chem. Soc.* **137,** 4594–4597 CrossRef Medline
47. Hynes, R. O. (2009) The extracellular matrix: Not just pretty fibrils. *Science* **326,** 1216–1219 CrossRef Medline
48. Wieslander, J., Langeveld, J., Butkowski, R., Jodlowski, M., Noelken, M., and Hudson, B. G. (1985) Physical and immunochemical studies of the globular domain of type IV collagen. Cryptic properties of the Goodpasture antigen. *J. Biol. Chem.* **260,** 8564–8570 Medline
49. Langeveld, J. P., Wieslander, J., Timoneda, J., McKinney, P., Butkowski, R. J., Wisdom, B. J., Jr., and Hudson, B. G. (1988) Structural heterogeneity of the noncollagenous domain of basement membrane collagen. *J. Biol. Chem.* **263,** 10481–10488 Medline
50. Chen, H. J., and Chiu, W. L. (2008) Simultaneous detection and quantification of 3-nitrotyrosine and 3-bromotyrosine in human urine by stable isotope dilution liquid chromatography tandem mass spectrometry. *Toxicol. Lett.* **181,** 31–39 CrossRef Medline
51. Filbey, K. J., Camberis, M., Chandler, J., Turner, R., Kettle, A. J., Eichenberger, R. M., Giacomin, P., and Le Gros, G. (2019) Intestinal helminth infection promotes IL-5- and $CD4^+$ T cell-dependent immunity in the lung against migrating parasites. *Mucosal Immunol.* **12,** 352–362 CrossRef Medline